DOI: 10.1002/ejic.200700369

A Hexadecanuclear Copper(I)–Copper(II) Mixed-Valence Compound: Structure, Magnetic Properties, Intervalence Charge Transfer, EPR, and NMR

Senjuti De,[a] Shubhamoy Chowdhury,[a] Jnan P. Naskar,[a] Michael G. B. Drew,[b] Rodolphe Clérac,[c] and Dipankar Datta*[a]

Keywords: Copper / High-nuclearity complexes / Aggregates / Mixed-valent compounds / Charge transfer / N,O ligands

Hexadecanuclear copper mixed-valence complex **2** containing 10 Cu^{II} centers and 6 Cu^{I} centers was isolated with N,O donor ligands. From the X-ray crystal structure, **2** was found to contain a centrosymmetric dimeric cation – each monomeric unit composed of eight copper centers. It displays a very broad and weak intervalence charge-transfer band around 1100 nm at room temperature in the solid state. Variable-temperature magnetic susceptibility measurements indicate an $S = 1/2$ ground state for half of **2**, explicitly, each Cu_8 moiety has a g value around 2.26. Complex **2** was examined by NMR spectroscopy at room temperature in solution and by EPR at low temperature; the data indicates that the valence is delocalized in **2** at room temperature but localized at low temperature.

Introduction

High-nuclearity ($n > 10$) metal complexes are of much current interest as these may have applications in catalysis, bio- and nanotechnology, material science, and molecular magnetism. The most impressive example is possibly $[Mn_{84}O_{72}(CH_3COO)_{78}(CH_3O)_{24}(CH_3OH)_{12}(OH)_6(H_2O)_{42}]\cdot x H_2O\cdot y CHCl_3$, which is a single molecule magnet of nano dimension.[1] The highest nuclearity n has so far been achieved in the case of Mo (n = 368).[2] This n may depend on the oxidation state of the metal. For example, the highest n reported to date for Cu^{I} is 146,[3] whereas it is 44 in the case of Cu^{II}.[4] Further, the situation might change in mixed-valence compounds. The highest n reported so far for Cu^{I}–Cu^{II} mixed-valence compounds is 38; this complex is made up of 36 Cu^{II} centers and 2 Cu^{I} centers.[5] A somewhat old review on high nuclearity Cu^{I}–Cu^{II} mixed-valence complexes is available.[6] A general interesting feature of the mixed-valence complexes is the appearance of an intervalence charge-transfer (ICT) band in the electronic spectra.[7–9] However, such a band was not observed so far in any Cu^{I}–Cu^{II} mixed-valence complex with $n > 3$. Herein we describe an air stable Cu^{I}–Cu^{II} mixed-valence complex with n = 16 that displays the rare ICT band.

[a] Department of Inorganic Chemistry, Indian Association for the Cultivation of Science,
Calcutta 700 032, India
Fax: +91-33-2473-2805
E-mail: icdd@mahendra.iacs.res.in
[b] School of Chemistry, University of Reading,
Whiteknights, Reading RG6 6AD, UK
[c] Université Bordeaux 1, CNRS, Centre de Recherche Paul Pascal – UPR8641,
115 avenue du Dr. A. Schweitzer, 33600 Pessac, France
Supporting information for this article is available on the WWW under http://www.eurjic.org or from the author.

Previously we reported[10] a hexanuclear Cu^{II} complex of LH (H: dissociable proton; Scheme 1), the acetone condensate of L′H (3-hydrazono-butan-2-one oxime; Scheme 1), of the formulation $Cu_6L_6(O)(OH)(ClO_4)_3$ (**1**). Its X-ray crystal structure was also reported. It is a H-bonded, centrosymmetric dimer of a centrally μ_3-oxido bridging Cu_3 complex cation $[Cu_3L_3(O)]^{2+}$ having peripheral oximato bridges. We have now found that if the crystallization of **1** is delayed in its synthesis, **1** is transformed into unique hexadecanuclear mixed-valence Cu^{I}–Cu^{II} complex **2**. Its X-ray crystal structure, spectroscopic (electronic and magnetic resonance), and magnetic properties are described here.

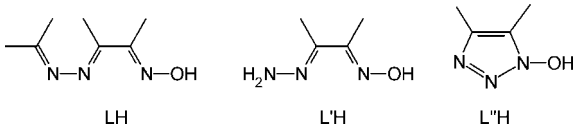

Scheme 1. Some ligands involved in the present work; H: dissociable proton.

Results and Discussion

The unit cell of **2** contains a centrosymmetric dimer of formula $[Cu_{16}L_2L'_2L''_{16}(H_2O)_2]^{6+}$ together with 6 discrete perchlorate anions and 10 solvent water molecules. Thus, the molecular formula of **2** is $[Cu_{16}L_2L'_2L''_{16}(H_2O)_2](ClO_4)_6\cdot 10H_2O$. The cation shown in Figure 1 contains eight independent copper atoms, all with different environments; Cu1, Cu6, and Cu7 are tetrahedral, Cu2 is four-coordinate square planar, Cu3 and Cu4 are five-coordinate square pyramidal, Cu5 is two-coordinate linear, and Cu8 is three-coordinate trigonal. The numbering scheme is such that the

ligands are numbered 1–10 inclusive with each atom numbered by the ligand number first and then the position of the atom in the ligand; L′′ is numbered 1–8 inclusive, with L′ numbered 9 and L numbered 10. In ligand L′′, three atoms, namely N*n*1, N*n*2 and O*n*5 are found to bind to copper atoms. The acyclic ligands L and L′ both chelate to one copper atom but also bind to other copper atoms through their other available donor atoms.

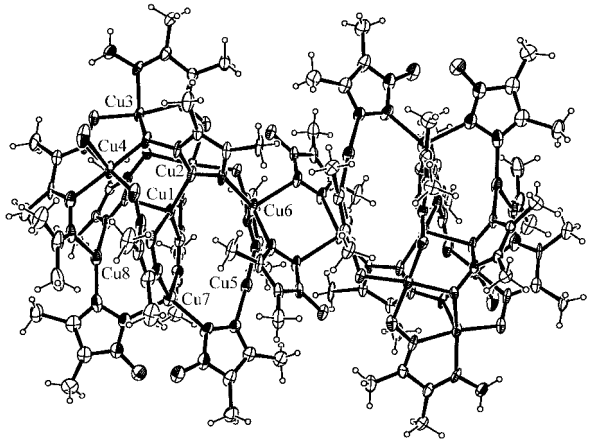

Figure 1. The structure of the centrosymmetric, dimeric cation in **2** with ellipsoids at 10% probability.

The environment of Cu1, shown in Figure 2; it is four-coordinate tetrahedral in which the metal atom is bound to four ligands through their central nitrogen atom N*n*1, where *n* is 1, 2, 7, and 8. The environment of Cu2 by contrast is four-coordinate square planar in which the metal atom is bonded to four ligands through the terminal oxygen atom O*n*5 where *n* is 5, 7, 8, and 9 (Figure 3). There is, in addition, a weak interaction with a perchlorate oxygen atom O21 at 2.53(1) Å. The environment of Cu3 is a five-coordinate square pyramid with O15 in an axial position and O105 and O85 together with the two nitrogen atoms N95 and N92 from the bidentate ligand L′ in the equatorial plane (Figure 4). Cu4 also has a five-coordinate square pyramidal geometry, but here a water molecule is in an axial position with O15 and O25 as well as two nitrogen atoms N105 and N102 from the bidentate L (Figure 5). The Cu5 atom is two-coordinate linear (Figure 6) and is bonded to N42 and N52 at 1.878(11) and 1.886(11) Å. The N42–Cu5–N52 angle is 173.4(5)°. There are no other bonding interactions for Cu5. The Cu6 atom has a tetrahedral environment but unlike Cu1 it is bonded to two N*n*1 atoms and two N*n*2 atoms. The Cu6 atom is involved in the centrosymmetric bridge as shown in Figure 7. The Cu7 atom is also tetrahedral and similar to Cu6, which is bonded to a combination of N*n*1 and N*n*2 atoms as shown in Figure 8. The Cu8 atom is three-coordinate trigonal and is bonded to N32, N82, and N101 as shown in Figure 9. Overall, the closest Cu···Cu distance in the cation $[Cu_{16}L_2L'_2L''_{16}(H_2O)_2]^{6+}$ is 3.114 Å between Cu1 and Cu2, indicating that there are no significant bonding interactions between copper atoms.

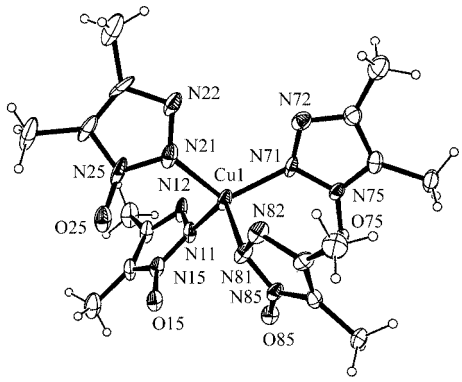

Figure 2. The environment of Cu1 with ellipsoids at 25% probability. Selected bond lengths [Å] and angles [°]: Cu1–N71 1.965(10), Cu1–N11 1.965(11), Cu1–N21 2.067(12), Cu1–N81 2.154(9), N71–Cu1–N11 135.2(4), N71–Cu1–N21 108.7(5), N11–Cu1–N21 105.9(4), N71–Cu1–N81 90.3(4), N11–Cu1–N81 112.2(4), N21–Cu1–N81 98.0(4).

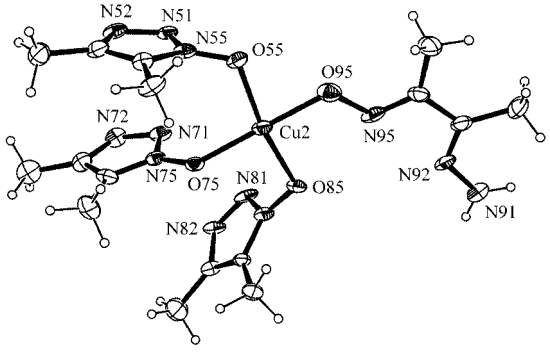

Figure 3. The environment of Cu2 with ellipsoids at 25% probability. Selected bond lengths [Å] and angles [°]: Cu2–O95 1.921(9), Cu2–O75 1.923(8), Cu2–O55 1.952(8), Cu2–O85 1.985(8), O95–Cu2–O75 170.2(4), O95–Cu2–O55 79.6(4), O75–Cu2–O55 97.0(3), O95–Cu2–O85 91.5(4), O75–Cu2–O85 92.6(3), O55–Cu2–O85 169.6(3).

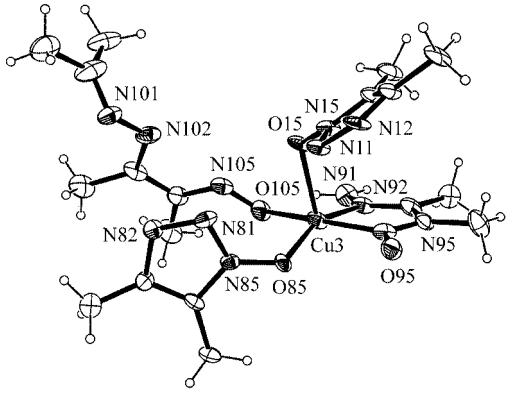

Figure 4. The environment of Cu3 with ellipsoids at 25% probability. Selected bond lengths [Å] and angles [°]: Cu3–O105 1.902(9), Cu3–N95 1.939(11), Cu3–N92 1.965(11), Cu3–O85 2.010(8), Cu3–O15 2.204(9), O105–Cu3–N95 170.4(5), O105–Cu3–N92 91.0(4), N95–Cu3–N92 79.9(5), O105–Cu3–O85 99.6(4), N95–Cu3–O85 87.9(4), N92–Cu3–O85 157.7(4), O105–Cu3–O15 88.8(4), N95–Cu3–O15 96.6(4), N92–Cu3–O15 105.2(4), O85–Cu3–O15 94.7(3).

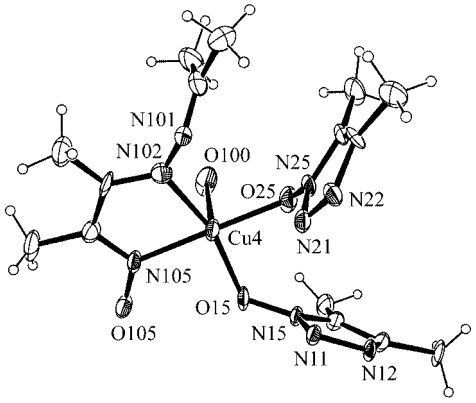

Figure 5. The environment of Cu4 with ellipsoids at 25% probability. O100 belongs to a water molecule. Selected bond lengths [Å] and angles [°]: Cu4–O25 1.914(10), Cu4–O15 1.950(10), Cu4–N105 2.007(10), Cu4–N102 2.014(13), Cu4–O100 2.313(10), O25–Cu4–O15 91.0(4), O25–Cu4–N105 179.2(5), O15–Cu4–N105 88.3(4), O25–Cu4–N102 102.5(5), O15–Cu4–N102 162.6(4), N105–Cu4–N102 78.3(5), O25–Cu4–O100 90.6(4), O15–Cu4–O100 95.8(4), N105–Cu4–O100 89.0(4), N102–Cu4–O100 94.9(4).

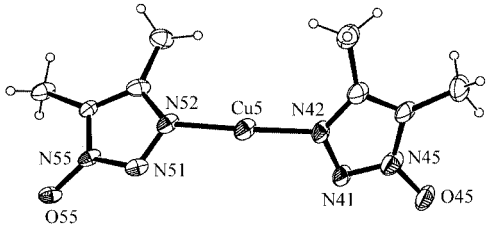

Figure 6. The environment of Cu5 with ellipsoids at 25% probability. Selected bond lengths [Å] and angles [°]: Cu5–N42 1.878(11), Cu5–N52 1.886(11), N42–Cu5–N52 173.4(5).

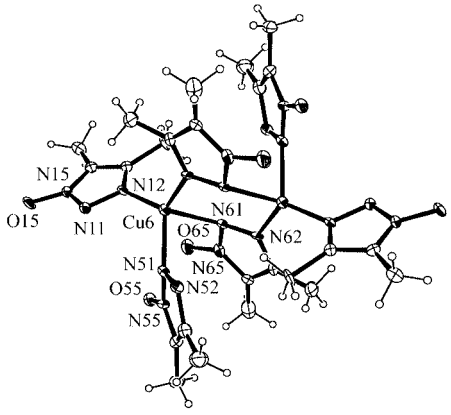

Figure 7. The environment of Cu6 with ellipsoids at 25% probability. The centrosymmetric bridge in the dimer is shown. Selected bond lengths [Å] and angles [°]: Cu6–N12 1.978(10), Cu6–N62$1 2.000(10), Cu6–N51 2.054(9), Cu6–N61 2.245(10), N12–Cu6–N62$1 125.6(4), N12–Cu6–N51 120.0(4), N62$1–Cu6–N51 105.0(4), N12–Cu6–N61 106.3(5), N62$1–Cu6–N61 102.8(4), N51–Cu6–N61 89.4(4).

We now discuss the binding nature of the three ligands occurring in **2** (Scheme 1). Of the three ligands, L and L′ are acyclic whereas L′′ is cyclic. The two acyclic ligands, L′ and L, chelate to one metal, N92 and N95 to Cu3, and

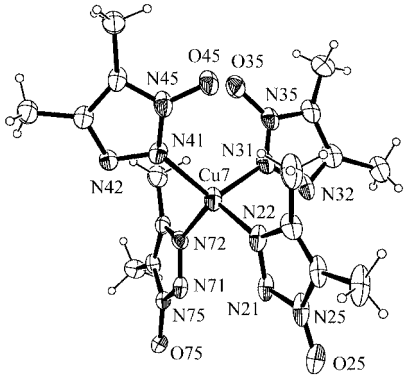

Figure 8. The environment of Cu7 with ellipsoids at 25% probability. Selected bond lengths [Å] and angles [°]: Cu7–N22 1.985(12), Cu7–N41 2.023(11), Cu7–N72 2.042(11), Cu7–N31 2.138(14), N22–Cu7–N41 122.1(5), N22–Cu7–N72 114.1(5), N41–Cu7–N72 104.1(4), N22–Cu7–N31 100.8(5), N41–Cu7–N31 113.1(5), N72–Cu7–N31 100.9(4).

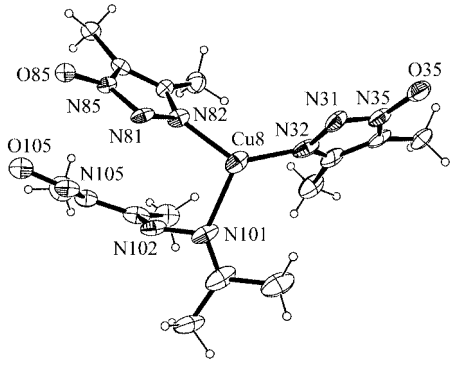

Figure 9. The environment of Cu8 with ellipsoids at 25% probability. Selected bond lengths [Å] and angles [°]: Cu8–N32 1.915(15), Cu8–N82 1.979(11), Cu8–N101 2.096(13), N32–Cu8–N82 130.3(5), N32–Cu8–N101 124.8(5), N82–Cu8–N101 102.8(5).

N102 and N105 to Cu4. In addition, O95 is bound to Cu2 within L′, N101 to Cu8, and O105 to Cu3 within L. There are eight types of L′′. Type 1 is bonded to four different metals: Cu1 through N11, Cu6 through N12, and Cu3 and Cu4 through O15. Type 2 is bonded to three copper atoms: Cu1 through N21, Cu7 through N22, and Cu4 through O25. Type 3 is bonded to two copper atoms: Cu7 through N31 and Cu8 through N32. Instead of bonding to a copper atom, O35 forms a strong hydrogen bond of 2.80 Å to solvent water O50. Type 4 is bonded to Cu7 through N41 and Cu5 through N42 but O45 remains unbonded. Type 5 is bonded to Cu6 through N51, Cu5 through N52, and Cu2 through O55. Type 6, which is adjacent to the center of symmetry, binds Cu6 through N61 and Cu61 through N62 (see Figure 7). Type 7 is bonded to Cu1 through N71, Cu7 through N72, and Cu2 through O75. Type 8 is bonded to Cu1 through N81, Cu8 through N82, and Cu2 and Cu3 through O85. Thus, for L′′, it can be concluded that its N*n*1 and N*n*2 are bound to different copper atoms, whereas its O*n*5 is bonded to two, one, or no copper atoms.

The formulation of complex **2** indicates that it consists of 10 Cu^{II} and 6 Cu^{I} centers. To assign the oxidations states

of various copper centers in **2**, we take recourse to the bond valence sum (BVS) model. BVS relates the bond lengths around a metal center to its oxidation state. In this method, originally introduced by Pauling and developed later by Brown and coworkers,[11–13] the valence v_{ij} of a bond between two atoms i and j is given empirically by Equation (1), where r_{ij} is the length (expressed in Å) and r_0 a parameter characteristic of the bond.

$$v_{ij} = \exp[(r_0 - r_{ij})/0.37] \quad (1)$$

The oxidation number V_i of an atom i is a simple algebraic sum of the v values of all the bonds formed by the atom [Equation (2)]; it is also known as BVS.

$$V_i = \sum_j v_{ij} = \sum_j \exp[(r_0 - r_{ij})/0.37] \quad (2)$$

Thus, if r_0 is known for a particular bond type the BVS can be calculated from the crystallographically determined r_{ij} values. The r_0 values for Cu^{II}–N and Cu^{II}–O bonds, as refined by us,[12] are 1.719 and 1.679 Å, respectively. Previously, we found[12] that with these r_0 values, the BVS values calculated for a number of Cu^{II} complexes of N and O donor ligands are found to lie in the range of 2.00 ± 0.35 valence units, specifically, the oxidation number of copper in these complexes are reproduced within ± 0.35 valence units. When we apply this method to **2**, we obtain the following BVS values for the eight types of copper atoms: Cu1, 1.73; Cu2, 1.95; Cu3, 2.26; Cu4, 2.10; Cu5, 1.29; Cu6, 1.61; Cu7, 1.67; and Cu8, 1.44. Thus our BVS calculations show that in the cases of Cu5, Cu6, and Cu8, the errors in the calculated oxidation states by assuming an oxidation state of II for all the copper atoms, exceed our stipulated error limit of ± 0.35 valence units. Consequently, an oxidation state of I is assigned to Cu5, Cu6, and Cu8 and an oxidation state of II to other five copper centers, namely Cu1, Cu2, Cu3, Cu4, and Cu7.

In the synthesis of complex **2** from complex **1**, L is transformed to L′ and L′′. L′ is generated from L by simple hydrolysis of the acetone azine bond. Ligand L′ is then subsequently transformed into L′′. A tentative mechanism for this transformation in methanol (a protic solvent) is suggested in Scheme 2. It involves a two-electron oxidation in the last step. We believe this oxidation is brought about by two Cu^{II} centers because the reaction **1**→**2** occurs under a N_2 atmosphere as well, and thereby some of the Cu^{II} centers are reduced to Cu^{I}, which leads to the formation of a mixed-valence species. Interestingly, in the synthesis of [1,2,3]triazol-1-ol (the basic skeleton in L′′H) from glyoxal, proposed by Begtrup, a similar oxidation by Cu^{2+} occurs in the last step.[14] X-ray crystal structures of a few of its derivatives are available. However, metal complexes of [1,2,3]triazol-1-ol are so far not known in the literature. Complex **2** illustrates the hitherto unexplored coordination behavior of [1,2,3]triazole-1-ol.

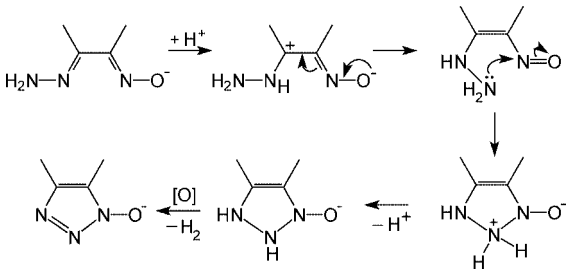

Scheme 2. A proposed mechanism for the chemical transformation of L′ into L′′ in a protic solvent.

Variable-temperature magnetic susceptibility (χ) of **2** was measured and is shown in Figure 10 as a χT versus T plot. At room temperature, χT is 0.89 $cm^3 \cdot K \cdot mol^{-1}$ and slowly decreases to 0.85 $cm^3 \cdot K \cdot mol^{-1}$ at 210 K. The value of χT is found to be roughly constant in the temperature range 210–100 K. Then it again decreases down to an asymptotic value of 0.48 $cm^3 \cdot K \cdot mol^{-1}$ at 1.85 K. On the basis of the molecular structure of complex **2** (Figure 1), we tried to simplify the topology of the Cu_{16} aggregate in order to analyze the magnetic behavior theoretically. The centrally located four diamagnetic Cu^{I} centers magnetically isolate the Cu^{II} ions into two distinct Cu^{II}_5 units (see the inset in Figure 10). In each such unit, at least four different types of magnetic interactions are present and were considered to model the magnetic property in the framework of Heisenberg's theory. However, all our attempts in this regard were unsuccessful due to the incapacity to evaluate the strong antiferromagnetic interaction between $S = 1/2$ Cu^{II} metal ions present in a part of the Cu^{II}_5 units (likely through direct oxygen bridges). Unfortunately, the limited available temperature range between 210 and 300 K did not allow an accurate estimation of these strong interactions. The decrease in the χT product below 100 K reveals that there are additional and weaker antiferromagnetic interactions in the Cu^{II}_5 units. Even if the amplitude of these interactions is not possible to determine, the asymptotic χT value of 0.48 $cm^3 \cdot K \cdot mol^{-1}$ observed at 1.85 K suggests an $S = 1/2$ ground state for a Cu_8 unit with a g value around 2.26.

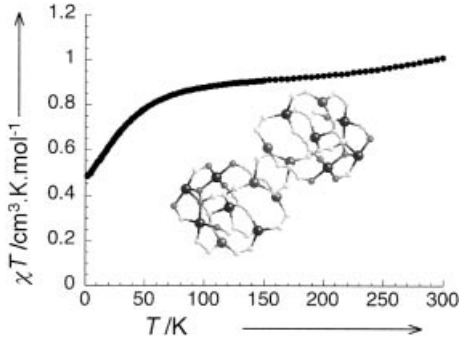

Figure 10. Temperature dependence of the χT product at 1000 Oe (where $\chi = M/H$) for half of $[Cu_{16}L_2L'_2L''_{16}(H_2O)_2](ClO_4)_6 \cdot 10H_2O$ (**2**) shown schematically in the inset.

Complex **2** displays a very broad and weak band around 1100 nm in the solid state at room temperature (Figure 11). This band could not be observed in methanol solution at

room temperature. However, relative to the intensity of the 650 nm band (Figure 11), which is very well observed in methanol solution, it appears that the intensity of the 1100 nm band is much less than 2900 $M^{-1}\cdot cm^{-1}$. No copper(II) or copper(I) complex is known in the literature that displays an absorption band at such a long wavelength. We ascribe this band to an intervalence charge transfer in **2**. It is difficult to specify how many copper centers are actually involved in the intervalence charge transfer. It is possible that two-coordinate Cu5 and three-coordinate Cu8 are not involved in the intervalence charge transfer process because of geometric reasons. One of the criteria for facile intervalence charge transfer is that the coordination environments (geometries and the binding atoms) of metal centers in the two oxidation states should be close to each other.[7–9] The four-coordinate copper(I) center Cu6 is directly bridged to two four-coordinate copper(II) centers Cu1 and Cu2. Of these two, Cu1 has a distorted tetrahedral N_4 and Cu2 ha a square planar O_4 coordination sphere. Thus, geometrywise and in terms of the nature of the binding atoms, the copper(I) center Cu6 seems to be compatible only with the copper(II) center Cu1 for the involvement in the ICT process. Previously in a binuclear mixed-valence Cu^{I}–Cu^{II} complex where both the copper centers have N_2O_2 coordination sphere, Long and Hendrickson[15] have observed a broad ICT band at 950 nm with an intensity of 400 $M^{-1}\cdot cm^{-1}$ in solution at room temperature.

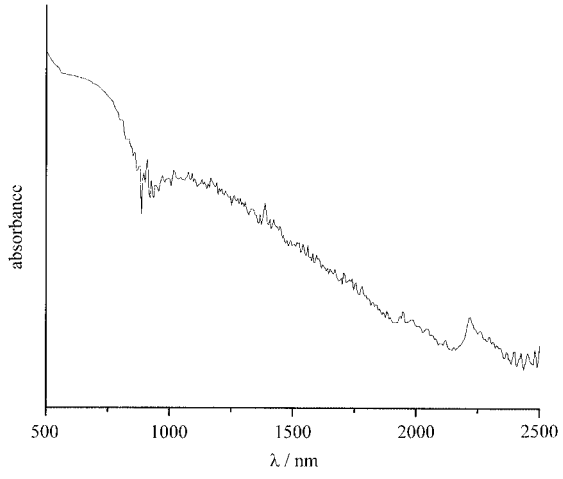

Figure 11. A portion of the absorption spectrum of **2** in nujol at room temperature.

The extensive valence delocalization in the complex of Long and Hendrickson at room temperature was established by the observation of a seven-line EPR spectrum in solution. Interestingly, their complex gives an EPR spectrum characteristic of a mononuclear copper(II) center at 100 K, to be exact, with the lowering of temperature valence gets localized.[15] In our case, valence delocalization renders the EPR signal so broad that we do not see any EPR spectrum at room temperature either in the solid state (Figure 12) or in solution. However, at low temperature (5 K) **2** displays an unsymmetrical spectrum with a *g* value of ca. 2.12. Thus in complex **2** valence is also delocalized at room temperature and localized at low temperature. The nonobservance of an EPR spectrum for **2** in methanol solution at room temperature despite being paramagnetic is supported by the observation of its ^1H NMR spectrum in CD_3OD at room temperature (Figure 13). Resonances due to the various methyl and NH_2 groups and water molecules present in **2** appear within the range –5 to 15 ppm. As expected, the ^1H signals are somewhat broad (Figure 13).

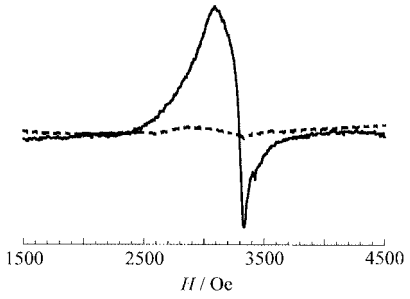

Figure 12. X-band EPR spectrum of **2** in solid state at 300 (dashed line) and 5 (full line) K.

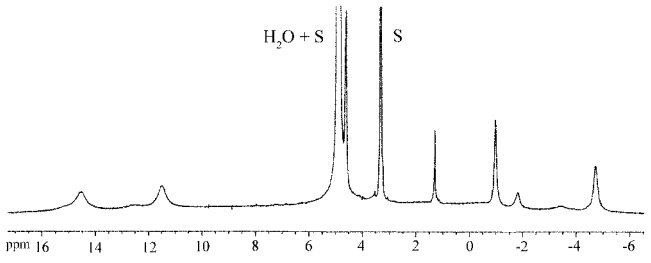

Figure 13. 300 MHz ^1H NMR spectrum of **2** in CD_3OD; peaks marked by S are due to solvent.

Concluding Remarks

Here we have described a unique, self-assembled, paramagnetic cluster containing copper(I) and copper(II) that displays NMR in solution at room temperature and EPR at low temperature. Such magnetic resonance behavior only suggests that valence is delocalized in complex **2** at room temperature but localized at lower temperatures. This sort of valence localization–delocalization is expected intuitively. On reaching sufficiently low temperatures, a delocalized (ambient-temperature) system gets *trapped in a valence-localized state*.[16,17] Accordingly, an intervalence charge-transfer band is also observed for **2** at room temperature at a low energy (1100 nm). In Hush theory,[18,19] for a class II (valence localized) system the observed bandwidth should be close to $(2310 \times \tilde{\nu}_{max})^{1/2}$ cm^{-1}; when the experimental bandwidth is much lower than the calculated one, the system becomes class III (complete valence delocalization). With λ_{max} = 1100 nm, the half-width is calculated to be 4600 cm^{-1}. Unfortunately, because of an intense neighboring band in the absorption spectrum of **2**, we cannot ascertain the exact half-width of the 1100 nm band experimentally, thus preventing us to categorize mixed valence complex **2** in terms of Hush theory. Self-assembly, which is

an important phenomenon in nature, has been a matter of extensive research in recent times.[20,21] Here it has assumed a different dimension.

Experimental Section

General: Microanalyses were performed with a Perkin–Elmer 2400II elemental analyzer. FTIR spectra (KBr disc) were recorded with a Shimadzu FTIR-8400S spectrophotometer, UV/Vis/NIR spectra with a Perkin–Elmer Lambda 950 spectrophotometer, and NMR spectra with a Bruker DPX300 spectrometer. The magnetic susceptibility measurements were obtained with the use of a Quantum Design SQUID magnetometer MPMS-XL. This magnetometer works between 1.8 and 400 K for dc applied fields ranging from –7 to 7 T. Measurements were performed on finely ground crystalline samples of 31.36 mg. M vs. H measurements were performed at 100 K to check for the presence of ferromagnetic impurities that were found to be absent. The magnetic data were corrected for the sample holder and the diamagnetic contribution.

Synthesis of 1: Prepared by modifying the previously published procedure[10] in the following manner. $Cu(ClO_4)_2{\cdot}6H_2O$ (1.86 g, 5 mmol) dissolved in methanol (10 mL) was added dropwise to LH (0.77 g, 5 mmol) and anhydrous sodium acetate (0.41 g, 5 mmol), dissolved in methanol (20 mL), with stirring. A dark green compound started precipitating immediately. Stirring was continued for only 2 min. Then the compound was filtered, washed with cold methanol (5 mL) and dried in air. Yield: 0.4 g (30%).

Synthesis of 2: Complex **1** (0.53 g, 0.32 mmol) was dissolved in methanol (100 mL) in a conical flask to obtain a clear green solution and layered with diethyl ether (300 mL), stoppered, and left undisturbed. After three weeks, the precipitated green crystalline compound was filtered and washed with diethyl ether (single crystals suitable for X-ray crystallography were found at the upper portion). It was dried under vacuum over fused $CaCl_2$. Yield: 0.35 g (65%). Λ_M (MeOH): 591 $\Omega^{-1}{\cdot}cm^2{\cdot}mol^{-1}$. FTIR (KBr): $\tilde{\nu}$ = 3447 (vb) ν(OH), 1117 (vs), 629 (s) $\nu(ClO_4)$ cm^{-1}. UV/Vis/NIR (MeOH): λ (ε, $M^{-1}{\cdot}cm^{-1}$) = 203 (10.5×10^5), 263 (14.3×10^4), 322 (10.9×10^4), 642 (2.9×10^3) nm. $C_{86}H_{160}Cl_6Cu_{16}N_{60}O_{56}$ (4160.01): calcd. C 24.81, H 3.88, N 20.20; found C 24.70, H 3.96, N 20.03.

Caution! Though we have not met with any incident during our studies, care should be taken in handling these compounds as perchlorate salts are potentially explosive. These should not be prepared and stored in larger amounts.

X-ray Crystallography: Data for **2** were collected at 150 K with a Bruker SMART APEX CCD diffractometer using graphite monochromated Mo-K_α radiation (λ = 0.71073 Å). Data reduction was performed with SAINT+[22] and absorption corrections applied using SADABS.[23] The structure was solved by direct methods[24] and refined[25] on F^2 using SHELX97. All non-hydrogen atoms were refined anisotropically and the hydrogen atoms were refined isotropically using a riding model. Of the three perchlorate anions in the asymmetric unit, two were refined with distance constraints. Five independent water molecules were located but their hydrogen atoms could not be located. Crystal Data: $C_{43}H_{80}Cl_3Cu_8N_{30}O_{28}$; M_r = 2080.04; triclinic; space group $P\bar{1}$; a = 13.898(4), b = 16.328(5), c = 18.642(6) Å; α = 82.144(6), β = 72.186(5), γ = 80.408(5)°; V = 3955(2) Å^3; Z = 2; $D_{calcd.}$ = 1.747 g·cm^{-3}. 18127 independent reflections were measured and were refined to R_1 0.1178, wR_2 0.2818 for 7300 reflections with $I>2\sigma(I)$. CCDC-600589 contains the supplementary crystallographic data for this paper. These data can be obtained free of charge from the Cambridge Crystallographic Data Center via www.ccdc.cam.ac.uk/data_request/cif.

Supporting Information (see footnote on the first page of this article): Figure S1 showing the 300 MHz ^{1}H NMR of **2** in CD_3OD after shaking with D_2O.

[1] A. J. Tasiopoulos, A. Vinslava, W. Wernsdorfer, K. A. Abboud, G. Christou, *Angew. Chem. Int. Ed.* **2004**, *43*, 2117–2121.
[2] A. Müller, E. Beckmann, H. Bögge, M. Schmidtmann, A. Dvess, *Angew. Chem. Int. Ed.* **2002**, *41*, 1162–1167.
[3] H. Krautscheid, D. Fenske, G. Baum, M. Semmelmann, *Angew. Chem. Int. Ed. Engl.* **1993**, *32*, 1303–1305.
[4] M. Murugesu, R. Clérac, C. E. Anson, A. K. Powell, *Inorg. Chem.* **2004**, *43*, 7269–7271.
[5] M. Murugesu, R. Clérac, C. E. Anson, A. K. Powell, *Chem. Commun.* **2004**, 1598–1599.
[6] M. Dunaj-Jurco, G. Ondrejovic, M. Melnik, J. Garaj, *Coord. Chem. Rev.* **1988**, *83*, 1–28.
[7] M. B. Robin, P. Day, *Adv. Inorg. Chem. Radiochem.* **1967**, *10*, 247–422.
[8] P. N. Schatz in *Inorganic Electronic Structure and Spectroscopy*, (Eds.: E. I. Solomon, A. B. P. Lever), Wiley, New York, **1999**, vol. 2, pp. 175–226.
[9] D. M. D'Alessandro, F. R. Keene, *Chem. Soc. Rev.* **2006**, *35*, 424–440.
[10] P. Chakrabarti, V. G. Puranik, J. P. Naskar, S. Hati, D. Datta, *Indian J. Chem. Sect. A* **2000**, *39*, 571–578.
[11] I. D. Brown, D. Altermatt, *Acta Crystallogr., Sect. B* **1985**, *41*, 244–247.
[12] S. Hati, D. Datta, *J. Chem. Soc. Dalton Trans.* **1995**, 1177–1182.
[13] S. Nag, K. Banerjee, D. Datta, *New J. Chem.* **2007**, *31*, 832–834.
[14] P. Uhlmann, J. Felding, P. Vedsø, M. Begtrup, *J. Org. Chem.* **1997**, *62*, 9177–9181.
[15] R. C. Long, D. N. Hendrickson, *J. Am. Chem. Soc.* **1983**, *105*, 1513–1521.
[16] However, at times the converse is also observed. For example, Ward and coworkers reported a mixed-valence tricopper complex where spin delocalization occurs only below 120 K with the valence-localized form becoming more prevalent at higher temperatures.[17]
[17] P. L. Jones, J. C. Jeffery, J. P. Maher, J. A. McCleverty, P. H. Rieger, M. D. Ward, *Inorg. Chem.* **1997**, *36*, 3088–3095.
[18] N. S. Hush, *Prog. Inorg. Chem.* **1967**, *8*, 391–444.
[19] C. Creutz, *Prog. Inorg. Chem.* **1983**, *30*, 1–73.
[20] V. G. Machado, P. N. W. Baxter, J. M. Lehn, *J. Braz. Chem. Soc.* **2001**, *12*, 431–462.
[21] N. Ginseppone, J. L. Schmidt, J. M. Lehn, *J. Am. Chem. Soc.* **2006**, *128*, 16748–16763.
[22] *Area Detector control and Data Integration and Reduction Software*, Bruker AXS, Madison, MI, USA, **2001**.
[23] G. M. Sheldrick, *SADABS*, University of Göttingen, Göttingen, Germany, **1997**.
[24] G. M. Sheldrick, *Acta Crystallogr., Sect. A* **1990**, *46*, 467–473.
[25] G. M. Sheldrick, *SHELX-97, Program for Crystal Structure Refinement*, University of Göttingen, **1997**.

Received: April 4, 2007
Published Online: June 21, 2007

